Effect of sea-salt aerosol on tropospheric bromine chemistry

Lei Zhu[1], Daniel J. Jacob[1,2], Sebastian D. Eastham[3], Melissa P. Sulprizio[1], Xuan Wang[1], Tomás Sherwen[4,5], Mat J. Evans[4,5], Qianjie Chen[6,a], Becky Alexander[6], Theodore K. Koenig[7,8], Rainer Volkamer[7,8], L. Gregory Huey[9], Michael Le Breton[10,11], Thomas J Bannan[10], and Carl J. Percival[10,b]

[1]John A. Paulson School of Engineering and Applied Sciences, Harvard University, Cambridge, MA, USA
[2]Department of Earth and Planetary Sciences, Harvard University, Cambridge, MA, USA
[3]Laboratory for Aviation and the Environment, Massachusetts Institute of Technology, Cambridge, MA, USA
[4]Wolfson Atmospheric Chemistry Laboratories, Department of Chemistry, University of York, York, UK
[5]National Centre for Atmospheric Science (NCAS), University of York, York, UK
[6]Department of Atmospheric Sciences, University of Washington, Seattle, WA, USA
[7]Department of Chemistry, University of Colorado, Boulder, CO, USA
[8]Cooperative Institute for Research in Environmental Sciences (CIRES), Boulder, CO, USA
[9]School of Earth & Atmospheric Sciences, Georgia Tech, Atlanta, Georgia, USA
[10]The Centre for Atmospheric Science, School of Earth, Atmospheric and Environmental Sciences, University of Manchester, Simon Building, Brunswick Street, Manchester, M13 9PL, UK
[11]Department of Chemistry and Molecular Biology, University of Gothenburg, Medicinaregatan 9 C, 40530, Gothenburg, Sweden
[a]now at: Department of Chemistry, University of Michigan, Ann Arbor, MI, USA
[b]now at: Jet Propulsion Laboratory, California Institute of Technology, 4800 Oak Grove Drive, Pasadena, CA, USA

Correspondence to: Lei Zhu (leizhu@fas.harvard.edu)

Abstract. Bromine radicals influence global tropospheric chemistry by depleting ozone and OH, and by oxidizing elemental mercury, sulfur species, and volatile organic compounds. Observations typically indicate a 50% depletion of sea salt aerosol (SSA) bromide relative to seawater composition, implying that SSA debromination could be the dominant global source of tropospheric bromine. However, it has been difficult to reconcile this large source with the relatively low BrO concentrations observed in the marine boundary layer (MBL). Here we present a new mechanistic description of SSA debromination in the GEOS-Chem global atmospheric chemistry model with a detailed representation of halogen (Cl, Br, and I) chemistry. We show, for the first time, observed levels of SSA debromination can be reproduced in a manner consistent with observed BrO concentrations. Bromine radical sinks from the HOBr + S(IV) heterogeneous reactions and from ocean emission of acetaldehyde are found to be critical in moderating tropospheric BrO levels. The resulting HBr is rapidly taken up by SSA and also deposited. We find that the source of bromine radicals is mostly from SSA in the MBL, but from organobromines in the free troposphere. Simulated BrO in the MBL is generally much higher in winter than in summer due to a combination of greater SSA emission and weaker radiation. Outstanding issues are the model underestimate of free tropospheric BrO, driven by the HOBr + S(IV) reactions, and uncertainty regarding HBr uptake by SSA.

1 Introduction

Bromine radicals ($BrO_x \equiv Br + BrO$) influence global tropospheric chemistry by depleting the main oxidants (OH and ozone) and by oxidizing elemental mercury, reduced sulfur species, and volatile organic compounds (VOCs) (Saiz-Lopez and von Glasow, 2012; Simpson et al., 2015). Tropospheric bromine radical chemistry is initiated by the production of reactive

5 inorganic bromine (Br_y) from sea salt aerosol (SSA) debromination, decomposition of organobromines primarily of marine origin ($CHBr_3$, CH_2Br_2, and CH_3Br), and transport from the stratosphere. Within the Br_y family, bromine radicals cycle with non-radical reservoir species such as HBr, HOBr, $BrNO_2$, $BrNO_3$, Br_2, BrCl, and IBr. Loss of Br_y is by wet and dry deposition to the surface, mainly as HBr which is highly soluble in water.

10 Sea salt aerosol (SSA) is thought to be the largest source of tropospheric bromine. Observations show extensive debromination of SSA relative to seawater composition (Sander et al., 2003; Newberg et al., 2005). Parrella et al. (2012) estimate a global Br_y source of 1420 Gg Br a^{-1} from SSA debromination, as compared with 520 Gg a^{-1} from organobromines and 36 Gg a^{-1} from the stratosphere. Volatilization of bromide from SSA can take place by heterogeneous reactions with HOBr, HOCl, N_2O_5, ozone, and $ClNO_3$ (Vogt et al., 1996; Hirokawa et al., 1998; Keene et al., 1998; Firckert et al., 1999; von Glasow et al., 2002a,

15 b; Yang et al., 2005; Ordóñez et al., 2012; Saiz-Lopez et al., 2012; Long et al., 2014). A standing conundrum has been that observations of BrO in the marine boundary layer (MBL) do not show large enhancements relative to the free troposphere, where background concentrations are typically of the order of 1 ppt (Leser et al., 2003; Sander et al., 2003; Theys et al., 2011; Volkamer et al. 2015; Wang et al., 2015; Le Breton et al., 2017). Ozone observations in the MBL similarly do not show depletion that would be expected from high concentrations of BrO (de Laat and Lelieveld, 2000; Sherwen et al., 2016). This

20 has led recent global models to exclude SSA debromination as a source of Br_y (Schmidt et al., 2016; Sherwen et al., 2016).

Here we present a new mechanistic description of sea salt debromination in the GEOS-Chem global 3-D model of tropospheric chemistry including detailed representation of halogens (Cl, Br, and I) (Sherwen et al., 2016). We find that we can reproduce the observed levels of SSA debromination while also being consistent with the relatively low BrO concentrations observed in

25 the MBL. This is because the previously-recognized fast production of Br_y from SSA debromination is offset by fast removal Br atoms by oxygenated organics emitted from the ocean (Millet et al., 2010) and by fast removal of HOBr by dissolved SO_2 (S(IV)) in cloud droplets (Chen et al., 2017). In addition, we find little influence of SSA on free tropospheric Br_y because of efficient scavenging of both SSA and HBr. We examine the implications for the global budget of tropospheric bromine and tropospheric oxidants.

30 # 2 Data and methods

We use GEOS-Chem 12.0.0 (https://doi.org/10.5281/zenodo.1343547), which includes a detailed representation of ozone-NO_x-VOC-aerosol-halogen tropospheric chemistry (Sherwen et al., 2016). The model is driven by assimilated meteorological data for 2011–2012 from the Modern-Era Retrospective analysis for Research and Applications, Version 2 (MERRA2)

produced by the NASA Global Modeling and Assimilation Office (Gelaro et al., 2017). The horizontal resolution of MERRA2 is 0.5° × 0.625°, and is degraded here to 4° × 5° for input to GEOS-Chem. Dynamic and chemical time steps are 30 and 60 minutes, respectively. GEOS-Chem stratospheric chemistry as described by Eastham et al. (2014) is linearized following Murray et al. (2012) to serve as boundary conditions for stratospheric input to the troposphere. The model is spun up for 1 year

5 and we use simulation results for 2012.

Tropospheric bromine chemistry in GEOS-Chem was first introduced by Parrella et al. (2012). Loss of Br_y from the troposphere is mainly by deposition of HBr, which is highly water-soluble, unlike HOBr or BrO. Parrella et al. (2012) found that the acid-catalyzed $HOBr + Br^-$ aqueous-phase reaction in clouds and aerosols was critical for recycling bromide and maintaining

10 background tropospheric BrO at observed ~ 1 ppt levels:

$$HOBr\ (aq) + Br^- + H^+ \rightarrow Br_2\ (g) + H_2O \tag{R1}$$

$$Br_2 + h\nu \rightarrow 2\ Br \tag{R2}$$

$$Br + O_3 \rightarrow BrO + O_2 \tag{R3}$$

The most recent GEOS-Chem 12.0.0 includes a much broader consideration of heterogeneous bromine chemistry (Schmidt et

15 al., 2016), coupling to other halogens (Sherwen et al. 2016), the HOBr + S(IV) reactions in clouds (Chen et al., 2017), and oceanic emission of acetaldehyde which reacts rapidly with Br atoms (Millet et al., 2010).

Schmidt et al. (2016) and Sherwen et al. (2016) found that SSA debromination in GEOS-Chem caused excessive MBL BrO compared to observations. Chen et al. (2017) subsequently showed that the HOBr + S(IV) reactions in cloud water depletes

20 BrO by competing with the $HOBr + Br^-/Cl^-$ reactions:

$$HOBr\ (aq) + HSO_3^- \rightarrow H_2O + BrSO_3^- \tag{R4a}$$

$$HOBr\ (aq) + SO_3^{2-} \rightarrow OH^- + BrSO_3^- \tag{R4b}$$

$$BrSO_3^- + H_2O \rightarrow SO_4^{2-} + Br^- + 2H^+ \tag{R4c}$$

followed by HBr deposition. Oceanic acetaldehyde emission also partitions Br_y into HBr:

25 $$Br + CH_3CHO \rightarrow HBr + CH_2CHO \tag{R5}$$

This leads us to re-examine the impact of SSA debromination as a source of bromine radicals and the ability of the model to simulate relevant observations.

Emission of SSA to the atmosphere is through air bubbles bursting at the ocean surface, and positively depends on wind speed

30 (Monahan et al., 1986; Gong, 2003). The GEOS-Chem SSA simulation is based on Jaeglé et al. (2011) and separates fine (< 0.5 μm radius) and coarse SSA as two separate transported species. The global dry SSA source in our simulation is 3140 Tg a^{-1}. We emit bromide as part of fine and coarse SSA with a seawater ratio of 2.11×10^{-3} kg Br per kg dry SSA (Sander et al., 2003; Lewis and Schwartz, 2004), since observations show that fresh SSA has a bromide content equals that of seawater (Duce

and Woodcock, 1971; Duce and Hoffman, 1976; Turekian et al., 2003). SSA alkalinity is depleted by uptake of HNO_3 and SO_2 (Alexander et al., 2005).

Activation of SSA bromide takes place by heterogeneous reactions with HOBr, ozone, and $ClNO_3$ once alkalinity has been

5   titrated and SSA is acidified (Hirokawa et al., 1998; Keene et al., 1998; Fickert et al., 1999):

$$Br^- + HOBr\ (aq) + H^+ \rightarrow Br_2 + H_2O \tag{R1}$$

$$Br^- + O_3\ (aq) + H^+ \rightarrow HOBr + O_2 \tag{R6}$$

$$Br^- + ClNO_3\ (aq) + H^+ \rightarrow BrCl + HNO_3 \tag{R7}$$
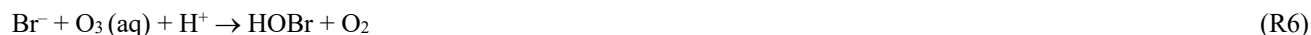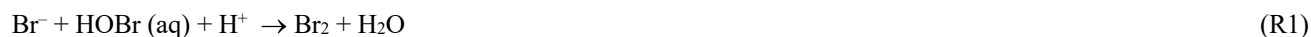
We also consider parameterized SSA debromination by HOI (aq) following McFiggans et al. (2002), where HOI (aq) may be

10   taken up from the gas phase or produced by hydrolysis of INO_2 and INO_3:

$$0.15Br^- + 0.85Cl^- + HOI\ (aq) + H^+ \rightarrow 0.15IBr + 0.85ICl + H_2O \tag{R8}$$
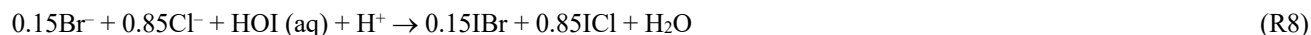
Inorganic oceanic iodine (HOI and I_2) emissions are from Carpenter et al. (2013). Unlike for chloride, SSA debromination does not take place by acid displacement because of the much stronger acidity of HBr than HCl or HNO_3 (Sander et al., 2003). On the contrary, uptake of gas-phase HBr can lead to bromine enrichment in SSA.

Sander et al. (2003) introduced the dimensionless enrichment factor (*EF*) as a measure of SSA debromination. *EF* is computed from aerosol measurements as:

$$EF = \frac{([Br^-]/[Na^+])_{measured}}{([Br^-]/[Na^+])_{seawater}} \tag{1}$$

where aerosol $[Na^+]$ is assumed to be mainly from sea salt, a reliable assumption in the marine air. In GEOS-Chem we treat

20   'SSA' as a chemically inert tracer, and account for sea-salt bromide as a separate species, therefore *EF* can be computed as:

$$EF = \frac{([Br^-]/[SSA])_{SSA\ aerosol}}{([Br^-]/[SSA])_{SSA\ emission}} \tag{2}$$

We sum $[Br^-]$ and [SSA] from both fine and coarse SSA to calculate *EF*.

3 Results and discussion

Figure 1 shows the annual mean SSA bromine enhancement factors (*EF*) in surface air computed by GEOS-Chem and

25   compares to annual mean observations compiled by Sander et al. (2003) and from Newberg et al. (2005). We consider 6 island and 4 coastal sites with bulk aerosol *EF* measurements available for more than one year. The observations are for different years than the GEOS-Chem simulation, but we assume that interannual variability is a minor source of error. The mean GEOS-Chem *EF* averaged over the sites is 0.68 ± 0.24 ($\pm$ 1 standard deviation), compared with the observed value of 0.66 ± 0.32. Global annual mean *EF* in GEOS-Chem is 0.60 ± 0.34. SSA bromide over the Southern Ocean in the model is less depleted

30   ($EF \sim 0.9$) than over the northern mid-latitudes ($EF \sim 0.5$), because GEOS-Chem SSA tends to retain its alkalinity over the

Southern Ocean (Alexander et al., 2005; Schmidt et al., 2016) thus preventing debromination via (R1) and (R6)–(R8). Similarly in the observations, mean *EF* is 0.78 ± 0.08 over the Southern Ocean compared with 0.42 ± 0.11 at northern mid-latitudes.

GEOS-Chem *EF* values are larger than unity (bromine enrichment) over some regions of the Southern Ocean and tropics, where SSA emissions are high. In these regions, high alkalinity emitted with SSA is not fully titrated due to limited supply of acids, resulting in non-depleted SSA bromide. On top of that, uptake of HBr on SSA leads to larger-than-unity *EF*. The very large bromine enrichment over the northwest coast of North America is due to large influx of SSA and Br$_y$ combined with the short lifetime of coarse SSA against deposition, so that Br$_y$ mobilized from coarse SSA is transferred to fine SSA as HBr. *EF* values drop further inland as Br$_y$ is remobilized from the fine SSA.

The model overestimates the observed *EF* over the Southern Ocean. This appears to reflect a seasonal bias. Figure 2 compares the simulated and observed seasonality at Cape Grim, Tasmania (Ayers et al., 1999; Sander et al., 2003). The observed *EF* is 0.6–0.8 for most of the year, consistent with the model, but decreases to below 0.4 in summer while the model does not. The summer minimum in the observations has been attributed to increased SSA acidity (Ayers et al., 1999; Sander et al., 2003). Indeed, Figure 2 shows that SSA alkalinity in the model is titrated in summer due to the combination of weaker SSA emission (lower winds) and larger photochemical production of strong acids (H$_2$SO$_4$ and HNO$_3$). This drives volatilization of Br$_y$ from SSA, but we find in the model that the resulting HBr mainly returns to SSA rather than deposits to the surface because SSA emission is still relatively high. Uptake of HBr by SSA in the model proceeds with an uptake coefficient $\gamma = 1.3 \times 10^{-8}$ exp(4290 K / T) as recommended by IUPAC (Amman et al., 2013) but uncertainty is large, ranging from –90% to +860% at 278 K.

Figure 3 shows the global budget and speciation of tropospheric Br$_y$. This updates a similar figure (Fig. 1 therein) by Schmidt et al. (2016) to include SSA debromination, the HOBr + S(IV) reactions in clouds, oceanic emission of acetaldehyde, and full coupling with the other halogens. SSA debromination is the largest global source, mainly from (R1) and (R6) producing Br$_2$ and HOBr respectively. The dominant sink of Br$_y$ is uptake of HBr by SSA, rather than deposition, emphasizing the importance of competition between these two processes in determining the extent of SSA debromination.

Inclusion of SSA debromination increases the tropospheric Br$_y$ load by 60% (9.9 Gg Br) and the global annual mean tropospheric BrO by 45% (0.09 ppt). Global tropospheric annual mean ozone and OH is reduced by 4.0% (1.3 ppb) and 2.3%, respectively. The principal global sink of Br$_y$ is uptake of HBr by SSA followed by SSA deposition. The dominant form of Br$_y$ is HBr (21% of Br$_y$), unlike HOBr in Schmidt et al. (2016), due to the global effect of (R4) and (R5). Despite our inclusion of the SSA debromination source, the global mean tropospheric Br$_y$ mixing ratio is decreased to 1.9 ppt as compared with 3.0 ppt in Schmidt et al. (2016). This is caused by the larger fraction of Br$_y$ present as HBr and therefore removed efficiently by uptake by SSA as well as by deposition. The global mean tropospheric BrO mixing ratio is 0.28 ppt as compared with 0.48 ppt in Schmidt et al. (2016). The daytime mixing ratio is about twice that value since BrO is depleted at night.

Figure 4 compares simulated tropospheric BrO columns with Global Ozone Monitoring Experiment (GOME)-2 satellite observations from Theys et al. (2011) as a function of season and for different latitudinal bands. SSA debromination increases the global annual mean tropospheric BrO column in our model by 46%. The largest effect is at extratropical latitudes in winter and spring due to a combination of higher SSA emissions and more effective bromide recycling via (R1). We find in the model

5 BrNO$_3$ hydrolysis becomes relatively more important in HOBr generation in winter and spring when BrNO$_3$ level is higher as a result of weaker photolysis. This leads to higher levels of HOBr, and therefore more effective recycling of bromide via (R1). Schmidt et al. (2016) previously found that their simulation including SSA debromination systematically overestimated the Theys et al. (2011) observations but we find the opposite because of (R4) and (R5) as discussed earlier. Chen et al. (2017) previously included (R4) and (R5) in GEOS-Chem with SSA debromination and found a mean low bias of 16% to 78% relative

10 to the GOME-2 data depending on latitudes. Similarly, the global mean bias is –44% in our simulation. The biases at high latitudes can be reduced by including a detail chlorine chemistry (Wang et al., 2018), since high chloride in those regions accelerate HOBr recycling by serving as a catalyst.

Figure 4 also shows tropospheric BrO columns measured in in Florida, USA (Coburn et al., 2011) and derived from mean

15 aircraft vertical profiles over the tropical Pacific from the TORERO (Volkamer et al., 2015; Wang et al., 2015; Dix et al., 2016) and CONTRAST (Koenig et al., 2017) campaigns. Values are consistent with the GOME-2 data of Theys et al. (2011). Figure 5 compares the simulated and observed vertical profiles. We see that the model low bias in the BrO column is mainly driven by the free troposphere, where SSA debromination plays little role and the Br$_y$ source is mainly from organobromines in the model. Schmidt et al. (2016) were far more successful at reproducing the observed vertical profiles but their simulation

20 did not include the HOBr + S(IV) reactions. We find in a sensitivity simulation without the HOBr + S(IV) reactions that free tropospheric BrO increases by a factor of three (Figure 5). The confined impact of SSA debromination on lower-altitude BrO as shown in Figure 5 is generally seen in other regions and seasons as well. Exceptions are for the extratropical latitudes in spring and winter, which is also reflected in BrO columns (Figure 4). In this case, the impact of SSA debromination extends through the depth of the troposphere. The explanation is that only ~ 20% of Br$_y$ there is present as HBr, reflecting the low

25 Br/BrO ratio when radiation is weak and hence the slower production of HBr by Br reactions (Figure 3). Br$_y$ has then a longer lifetime because non-HBr species are much less water-soluble (Parrella et al., 2012) and can be effectively transported to the free troposphere.

Figure 6 shows the simulated global distribution of BrO concentrations in surface air in January and July. We attribute the

30 elevated marine surface BrO in winter time to a combination of greater SSA emission and weaker radiation (lower Br/BrO ratio). However, we fail to find enough information in previous studies to verify the modeled seasonality in marine surface BrO. We are aware of only one site at Cape Verde (Read et al., 2008; Mahajan et al., 2010), which reports such seasonality, and they show a statistically insignificant difference between winter and summer time surface BrO. Daytime concentrations are twice the values shown in the Figure since BrO drops to near-zero at night. Observations are compiled in Table 1 with

35 corresponding model values. The model is generally consistent with observations in showing daytime concentrations in the

range 0.5–2 ppt. The low level of BrO (~ 0.3 ppt) over the eastern tropical Pacific Ocean (Chen et al, 2016) observed during the TORERO flight campaign is driven by weak SSA emission in the austral summer. The CONTRAST flight campaign took more readings over a region (near Guam) with higher SSA emission and load compared with CAST, resulting in higher level of BrO. The high biases of modeled surface BrO during CONTRAST and CAST may be due to the underestimate of cloud and aerosol pH. By using online aerosol pH calculation and reflecting SSA contribution to cloud pH, Wang et al. (2018) found much lower BrO concentrations in tropical Pacific Ocean. Both model and observations show high values (1.9–3.0 ppt) at Tenerife Island and Cape Verde in the tropical Atlantic. We attribute this to the elevated inorganic iodine emissions (HOI and I_2) in this region (Carpenter et al., 2013; Sherwen et al., 2016), which results in high Br_y and BrO in turn by activating SSA bromide via (R8). Isolated hotspots near India (July) and the Caribbean (January and July) correspond to localized hotspots of SSA emissions.

4 Conclusion

We have shown through GEOS-Chem model simulations that global observations of sea salt aerosol debromination generating bromine radicals can be reconciled with the relatively low observed BrO concentrations in the marine boundary layer due to the presence of several rapid bromine sinks. Sea salt aerosol debromination in the model is driven principally by HOBr + Br$^-$ and O_3 + Br$^-$ reactions, producing Br_2 and HOBr respectively, but the subsequent bromine radical cycling is limited by fast conversion to HBr through reactions of Br atoms with aldehydes (including acetaldehyde emitted by the ocean) and the heterogeneous HOBr + S(IV) heterogeneous reactions. In spite of the rapid removal of bromine, we find that inclusion of SSA debromination has a significant effect on tropospheric chemistry, lowering global tropospheric annual mean ozone by 4.0% and OH by 2.3%.

5 Acknowledgments

This work was supported by the NSF Atmospheric Chemistry Program. We acknowledge contributions from the TORERO, CONTRAST, and CAST science team. We thank Dexian Chen for the CONTRAST BrO observations. Q.C. and B.A. acknowledge support from NSF AGS 1343077.

6 Data availability

The GEOS-Chem model is available at http://acmg.seas.harvard.edu/geos/. Data are available upon request.

7 Author contributions

L.Z. and D.J.J. designed the research and wrote the paper; L.Z., D.J.J., S.D.E., M.P.S., X.W., T.S., M.J.E., Q.C., and B.A. led the model development; T.K.K., R.V., L.G.H., M.L., T.J.B., and C.J.P. provided BrO observations.

References

Alexander, B., Park, R. J., Jacob, D. J., Li, Q. B., Yantosca, R. M., Savarino, J., Lee, C. C. W., and Thiemens, M. H.: Sulfate formation in sea-salt aerosols: Constraints from oxygen isotopes, J. Geophys. Res., 110, D10307, doi:10.1029/2004JD005659, 2005.

Ammann, M., Cox, R. A., Crowley, J. N., Jenkin, M. E., Mellouki, A., Rossi, M. J., Troe, J., and Wallington, T. J.: Evaluated kinetic and photochemical data for atmospheric chemistry: Volume VI – heterogeneous reactions with liquid substrates, Atmos. Chem. Phys., 13, 8045–8228, https://doi.org/10.5194/acp-13-8045-2013, 2013.

Ayers, G. P., Gillett, R. W., Cainey, J. M., and Dick, A. L.: Chloride and bromide loss from sea-salt particles in southern ocean air, J. Atmos. Chem., 33, 299–319, 1999.

Carpenter, L. J., MacDonald, S. M., Shaw, M. D., Kumar, R., Saunders, R. W., Parthipan, R., Wilson, J., and Plane, J. M. C.: Atmospheric iodine levels influenced by sea surface emissions of inorganic iodine, Nature Geosci., 6, 108–111, doi:10.1038/ngeo1687, 2013.

Chen, D., Huey, L. G., Tanner, D. J., Salawitch, R. J., Anderson, D. C., Wales, P. A., Pan, L. L., Atlas, E. L., Hornbrook, R. S., Apel, E. C., Blake, N. J., Campos, T. L., Donets, V., Flocke, F. M., Hall, S. R., Hanisco, T. F., Hills, A. J., Honomichl, S. B., Jensen, J. B., Kaser, L., Montzka, D. D., Nicely, J. M., Reeves, J. M., Riemer, D. D., Schauffler, S. M., Ullmann, K., Weinheimer, A. J., and Wolfe, G. M.: Airborne measurements of BrO and the sum of HOBr and Br_2 over the Tropical West Pacific from 1 to 15 km during the CONvective TRansport of Active Species in the Trop- ics (CONTRAST) experiment, J. Geophys. Res.-Atmos., 121, 12560–12578, https://doi.org/10.1002/2016JD025561, 2016.

Chen, Q., Schmidt, J. A., Shah, V., Jaeglé, L., Sherwen, T., and Alexander, B.: Sulfate production by reactive bromine: Implications for the global sulfur and reactive bromine budgets, Geophys. Res. Lett., 44, 7069–7078, https://doi.org/10.1002/2017GL073812, 2017.

Coburn, S., Dix, B., Sinreich, R., and Volkamer, R.: The CU ground MAX-DOAS instrument: characterization of RMS noise limitations and first measurements near Pensacola, FL of BrO, IO, and CHOCHO, Atmos. Meas. Tech., 4, 2421–2439, https://doi.org/10.5194/amt-4-2421-2011, 2011.

de Laat, A. T. J. and Lelieveld, J.: The diurnal O3 cycle in the tropical and subtropical marine boundary layer, J. Geophys. Res., 105, 11 547–11 559, 2000.

Dix, B., Koenig, T. K., and Volkamer, R.: Parameterization retrieval of trace gas volume mixing ratios from Airborne MAX-DOAS, Atmos. Meas. Tech., 9, 5655–5675, https://doi.org/10.5194/amt-9-5655-2016, 2016.

Duce, R. A. and Hoffman, E.: Chemical fractionation at the air/sea interface, Annu. Rev. Earth Planet. Sci., 4, 187–228, 1976.

Duce, R. A. and Woodcock, A. H.: Difference in chemical composition of atmospheric sea salt particles produced in the surf zone and on the open sea in Hawaii, Tellus, 23, 427–435, 1971.

Eastham, S. D., Weisenstein, D. K., and Barrett, S. R. H.: Development and evaluation of the unified tropospheric–stratospheric chemistry extension (UCX) for the global chemistry-transport model GEOS-Chem, Atmos. Environ., 89, 52–63, doi:10.1016/j.atmosenv.2014.02.001, 2014.

Fickert, S., Adams, J.W., and Crowley, J. N.: Activation of Br_2 and BrCl via uptake of HOBr onto aqueous salt solutions, J. Geophys. Res., 104D, 23 719–23 727, 1999.

Gelaro, R., McCarty, W., Suárez, M. J., Todling, R., Molod, A., Takacs, L., Randles, C. A., Darmenov, A., Bosilovich, M. G., Re- ichle, R., Wargan, K., Coy, L., Cullather, R., Draper, C., Akella, S., Buchard, V., Conaty, A., da Silva, A. M., Gu, W., Kim, G.- K., Koster, R., Lucchesi, R., Merkova, D., Nielsen, J. E., Par- tyka, G., Pawson, S., Putman, W., Rienecker, M., Schubert, S. D., Sienkiewicz, M., and Zhao, B.: The Modern-Era Retrospective Analysis for Research and Applications, Version 2 (MERRA-2), J. Climate, 30, 5419–5454, https://doi.org/10.1175/JCLI-D-16-0758.1, 2017.

Gong, S. L.: A parameterization of sea-salt aerosol source func-tion for sub- and super- micron particles, Global Biogeochem. Cycles, 17(4), 1097, doi:1029/2003GB002079, 2003.

Hirokawa, J., Onaka, K., Kajii, Y., and Akimoto, H.: Heterogeneous processes involving sodium halide particles and ozone: Molecular bromine release in the marine boundary layer in the absence of nitrogen oxides, Geophys. Res. Lett., 25, 2449–2452, 1998.

Jaeglé, L., Quinn, P. K., Bates, T. S., Alexander, B., and Lin, J.-T.: Global distribution of sea salt aerosols: new constraints from in situ and remote sensing observations, Atmos. Chem. Phys., 11, 3137–3157, https://doi.org/10.5194/acp-11-3137–2011, 2011.

Keene,W. C., Sander, R., Pszenny, A. A. P., Vogt, R., Crutzen, P. J., and Galloway, J. N.: Aerosol pH in the marine boundary layer: A review and model evaluation, J. Aerosol Sci., 29, 339–356, 1998.

Keene, W. C., Stutz, J., Pszenny, A. A. P., Maben, J. R., Fis- cher, E. V., Smith, A. M., von Glasow, R., Pechtl, S., Sive, B. C., and Varner, R. K.: Inorganic chlorine and bromine in coastal New England air during summer, J. Geophys. Res., 112, D10S12, doi:10.1029/2006JD007689, 2007.

Koenig, T. K., Volkamer, R., Baidar, S., Dix, B., Wang, S., Anderson, D. C., Salawitch, R. J., Wales, P. A., Cuevas, C. A., Fernandez, R. P., Saiz-Lopez, A., Evans, M. J., Sherwen, T., Jacob, D. J., Schmidt, J., Kinnison, D., Lamarque, J.-F., Apel, E. C., Bresch, J. C., Campos, T., Flocke, F. M., Hall, S. R., Honomichl, S. B., Hornbrook, R., Jensen, J. B., Lueb, R., Montzka, D. D., Pan, L. L., Reeves, J. M., Schauffler, S. M., Ullmann, K., Weinheimer, A. J., Atlas, E. L., Donets, V., Navarro, M. A., Riemer, D., Blake, N. J., Chen, D., Huey, L. G., Tanner, D. J., Hanisco, T. F., and Wolfe, G. M.: BrO and inferred Bry profiles over the western Pacific: relevance of inorganic bromine sources and a Br$_y$ minimum in the aged tropical tropopause layer, Atmos. Chem. Phys., 17, 15245–15270, https://doi.org/10.5194/acp-17-15245-2017, 2017.

Le Breton, M, Bannan, T. J., Shallcross, D. E., Khan, M. A., Evans, M. J., Lee, J., Lidster, R., Andrews, S., Carpenter, L., Schmidt, J., Jacob, D., Harris, N. R. P., Bauguitte, S.-J., Gallagher, M., Bacak, A., Leather, K. E., and Percival, C. J.: Enhanced ozone loss by active inorganic bromine chemistry in the tropical troposphere, Atmos. Environ., 155, 21–28, 2017.

Leser,H.,Ho¨nninger,G.,andPlatt,U.:MAX-DOASMeasure- ments of BrO and NO₂ in the Marine Boundary Layer, Geophys. Res. Lett., doi:10.1029/2002GL015811, 2003.

Lewis, E. R., and S. E. Schwartz, Sea Salt Aerosol Production: Mechanisms, Methods, Measurements and Models—A Critical Review, AGU, 413 pp., Washington, D. C., 2004.

Long, M. S., Keene, W. C., Easter, R. C., Sander, R., Liu, X., Kerkweg, A., and Erickson, D.: Sensitivity of tropospheric chemical composition to halogen-radical chemistry using a fully coupled size-resolved multiphase chemistry–global climate system: halogen distributions, aerosol composition, and sensitivity of climate-relevant gases, Atmos. Chem. Phys., 14, 3397–3425, https://doi.org/10.5194/acp-14-3397-2014, 2014.

Mahajan, A. S., Plane, J. M. C., Oetjen, H., Mendes, L., Saunders, R. W., Saiz-Lopez, A., Jones, C. E., Carpenter, L. J., and McFiggans, G. B.: Measurement and modelling of tropospheric reactive halogen species over the tropical Atlantic Ocean, Atmos. Chem. Phys., 10, 4611–4624, https://doi.org/10.5194/acp-10-4611-2010, 2010.

Martin, M., Pöhler, D., Seitz, K., Sinreich, R., and Platt, U.: BrO measurements over the Eastern North-Atlantic, Atmos. Chem. Phys., 9, 9545–9554, https://doi.org/10.5194/acp-9-9545-2009, 2009.

McFiggans, G., Cox, R. A., Mossinger, J. C., Allan, B. J., and Plane, J. M. C.: Active chlorine release from marine aerosols: Roles for reactive iodine and nitrogen species, J. Geophys. Res.-Atmos., 107, ACH 10-1–ACH 10-13, doi:10.1029/2001jd000383, 2002.

Millet, D. B., Guenther, A., Siegel, D. A., Nelson, N. B., Singh, H. B., de Gouw, J. A., Warneke, C., Williams, J., Eerdekens, G., Sinha, V., Karl, T., Flocke, F., Apel, E., Riemer, D. D., Palmer, P. I., and Barkley, M.: Global atmospheric budget of acetaldehyde: 3-D model analysis and constraints from in-situ and satellite observations, Atmos. Chem. Phys., 10, 3405–3425, https://doi.org/10.5194/acp-10-3405-2010, 2010.

Monahan, E. C., Spiel, D. E., and Davidson, K. L.: A model of marine aerosol generation via whitecaps and wave disruption in oceanic whitecaps, in: Oceanic whitecaps and their role in air-sea exchange processes, edited by: Monahan, E. C. and Niocaill, G. M., D. Reidel Publishing, Dordrecht, Holland, 167–174, 1986.

Murray, L. T., Jacob, D. J., Logan, J. A., Hudman, R. C., and Koshak, W. J.: Optimized regional and interannual variability of lightning in a global chemical transport model constrained by LIS/OTD satellite data, J. Geophys. Res.-Atmos., 117, D20307, doi:10.1029/2012JD017934, 2012.

Newberg, J. T., Matthew, B. M., and Anastasio, C.: Chloride and bromide depletions in sea-salt particles over the northeastern Pacific Ocean, J. Geophys. Res., 110, D06209, doi:10.1029/2004JD005446, 2005.

Ordóñez, C., Lamarque, J.-F., Tilmes, S., Kinnison, D. E., Atlas, E. L., Blake, D. R., Sousa Santos, G., Brasseur, G., and Saiz-Lopez, A.: Bromine and iodine chemistry in a global chemistry-climate model: description and evaluation of very short-lived oceanic sources, Atmos. Chem. Phys., 12, 1423–1447, https://doi.org/10.5194/acp-12-1423-2012, 2012.

Parrella, J. P., Jacob, D. J., Liang, Q., Zhang, Y., Mickley, L. J., Miller, B., Evans, M. J., Yang, X., Pyle, J. A., Theys, N., and Van Roozendael, M.: Tropospheric bromine chemistry: implications for present and pre-industrial ozone and mercury, Atmos. Chem. Phys., 12, 6723–6740, https://doi.org/10.5194/acp-12-6723-2012, 2012.

Read, K. A., Mahajan, A. S., Carpenter, L. J., Evans, M. J., Faria, B. V. E., Heard, D. E., Hopkins, J. R., Lee, J. D., Moller, S. J., Lewis, A. C., Mendes, L., McQuaid, J. B., Oetjen, H., Saiz-Lopez, A., Pilling, M. J., and Plane, J. M. C.: Extensive

halogen-mediated ozone destruction over the tropical Atlantic Ocean, Nature, 453, 1232–1235, doi:10.1038/nature07035, 2008.

Saiz-Lopez, A., Plane, J. M. C., and Shillito, J. A.: Bromine oxide in the mid-latitude marine boundary layer, Geophys. Res. Lett., 31, doi:10.1029/2003GL018 956, 2004.

Saiz-Lopez, A., Shillito, J. A., Coe, H., and Plane, J. M. C.: Measurements and modelling of I₂, IO, OIO, BrO and NO₃ in the mid-latitude marine boundary layer, Atmos. Chem. Phys., 6, 1513–1528, https://doi.org/10.5194/acp-6-1513-2006, 2006.

Saiz-Lopez, A. and von Glasow, R.: Reactive halogen chem- istry in the troposphere, Chem. Soc. Rev., 41, 6448–6472, doi:10.1039/c2cs35208g, 2012.

Saiz-Lopez, A., Lamarque, J.-F., Kinnison, D. E., Tilmes, S., Ordóñez, C., Orlando, J. J., Conley, A. J., Plane, J. M. C., Mahajan, A. S., Sousa Santos, G., Atlas, E. L., Blake, D. R., Sander, S. P., Schauffler, S., Thompson, A. M., and Brasseur, G.: Estimating the climate significance of halogen-driven ozone loss in the tropical marine troposphere, Atmos. Chem. Phys., 12, 3939–3949, https://doi.org/10.5194/acp-12-3939-2012, 2012.

Sander, R., Keene, W. C., Pszenny, A. A. P., Arimoto, R., Ayers, G. P., Baboukas, E., Cainey, J. M., Crutzen, P. J., Duce, R. A., Hönninger, G., Huebert, B. J., Maenhaut, W., Mihalopoulos, N., Turekian, V. C., and Van Dingenen, R.: Inorganic bromine in the marine boundary layer: a critical review, Atmos. Chem. Phys., 3, 1301–1336, https://doi.org/10.5194/acp-3-1301-2003, 2003.

Simpson, W. R., Brown, S. S., Saiz-Lopez, A., Thornton, J. A., and von Glasow, R.: Tropospheric Halogen Chemistry: Sources, Cycling, and Impacts, Chem. Rev., 115, 4035–4062, doi:10.1021/cr5006638, 2015.

Schmidt, J. A., Jacob, D. J., Horowitz, H. M., Hu, L., Sherwen, T., Evans, M. J., Liang, Q., Suleiman, R. M., Oram, D. E., Le Breton, M., Percival, C. J., Wang, S., Dix, B., and Volkamer, R.: Modeling the observed tropospheric BrO background: Importance of multiphase chemistry and implications for ozone, OH, and mercury, J. Geophys. Res.-Atmos., 121, 11819–11835, doi:10.1002/2015JD024229, 2016.

Sherwen, T., Schmidt, J. A., Evans, M. J., Carpenter, L. J., Großmann, K., Eastham, S. D., Jacob, D. J., Dix, B., Koenig, T. K., Sinreich, R., Ortega, I., Volkamer, R., Saiz-Lopez, A., Prados-Roman, C., Mahajan, A. S., and Ordóñez, C.: Global impacts of tropospheric halogens (Cl, Br, I) on oxidants and composition in GEOS-Chem, Atmos. Chem. Phys., 16, 12239–12271, https://doi.org/10.5194/acp-16-12239-2016, 2016.

Theys, N., Van Roozendael, M., Hendrick, F., Yang, X., De Smedt, I., Richter, A., Begoin, M., Errera, Q., Johnston, P. V., Kreher, K., and De Mazière, M.: Global observations of tropospheric BrO columns using GOME-2 satellite data, Atmos. Chem. Phys., 11, 1791–1811, https://doi.org/10.5194/acp-11-1791-2011, 2011.

Turekian, V. C., Macko, S. A., and Keene, W. C.: Concentrations, isotopic compositions, and sources of size-resolved, particulate organic carbon and oxalate in near-surface marine air at Bermuda during spring, J. Geophys. Res., 108D, 4157, 10.1029/2002JD002 053, 2003.

Vogt, R., Crutzen, P. J., and Sander, R.: A mechanism for halogen release from sea-salt aerosol in the remote marine boundary layer, Nature, 383, 327–330, 1996.

Volkamer, R., Baidar, S., Campos, T. L., Coburn, S., DiGangi, J. P., Dix, B., Eloranta, E. W., Koenig, T. K., Morley, B., Ortega, I., Pierce, B. R., Reeves, M., Sinreich, R., Wang, S., Zondlo, M. A., and Romashkin, P. A.: Aircraft measurements of BrO, IO, glyoxal, NO₂, H₂O, O₂–O₂ and aerosol extinction profiles in the tropics: comparison with aircraft-/ship-based in situ and lidar measurements, Atmos. Meas. Tech., 8, 2121–2148, https://doi.org/10.5194/amt-8-2121-2015, 2015.

von Glasow, R., Sander, R., Bott, A., and Crutzen, P. J.: Modeling halogen chemistry in the marine boundary layer. 1. Cloud-free MBL, J. Geophys. Res., 107D, 4341, 10.1029/2001JD000 942, 2002a.

von Glasow, R., Sander, R., Bott, A., and Crutzen, P. J.: Modeling halogen chemistry in the marine boundary layer. 2. Interactions with sulfur and the cloud-covered MBL, J. Geophys. Res., 107D, 4323, 10.1029/2001JD000 943, 2002b.

Wang, S.-Y., Schmidtd, J., Baidar, S., Coburn, S., Dix, B., Koenig, T., Apel, E., Bowdalo, D., Campos, T., Eloranta, E., Evans, M., DiGangii, J., Zondlo, M., Gao, R.-S., Haggerty, J., Hall, S., Hornbrook, R., Jacob, D., Morley, B., Pierce, B., Reeves, M., Romashkin, P., ter Schure, A., and Volkamer, R.: Active and widespread halogen chemistry in the tropical and subtropical free troposphere, P. Natl. Acad. Sci. USA, 112, 9281–9286, doi:10.1073/pnas.1505142112, 2015.

Wang, X., Jacob, D. J., Eastham, S. D., Sulprizio, M. P., Zhu, L., Chen, Q., Alexander, B., Sherwen, T., Evans, M. J., Lee, B. H., Haskins, J. D., Lopez-Hilfiker, F. D., Thornton, J. A., Huey, G. L., and Liao, H.: The role of chlorine in tropospheric chemistry, Atmos. Chem. Phys. Discuss., https://doi.org/10.5194/acp-2018-1088, in review, 2018.

Yang, X., Cox, R., Warwick, N., Pyle, J., Carver, G., O'Connor, F., and Savage, N.: Tropospheric bromine chemistry and its impacts on ozone: A model study, J. Geophys. Res., 110, D23311, doi:10.1029/2005JD006244, 2005.
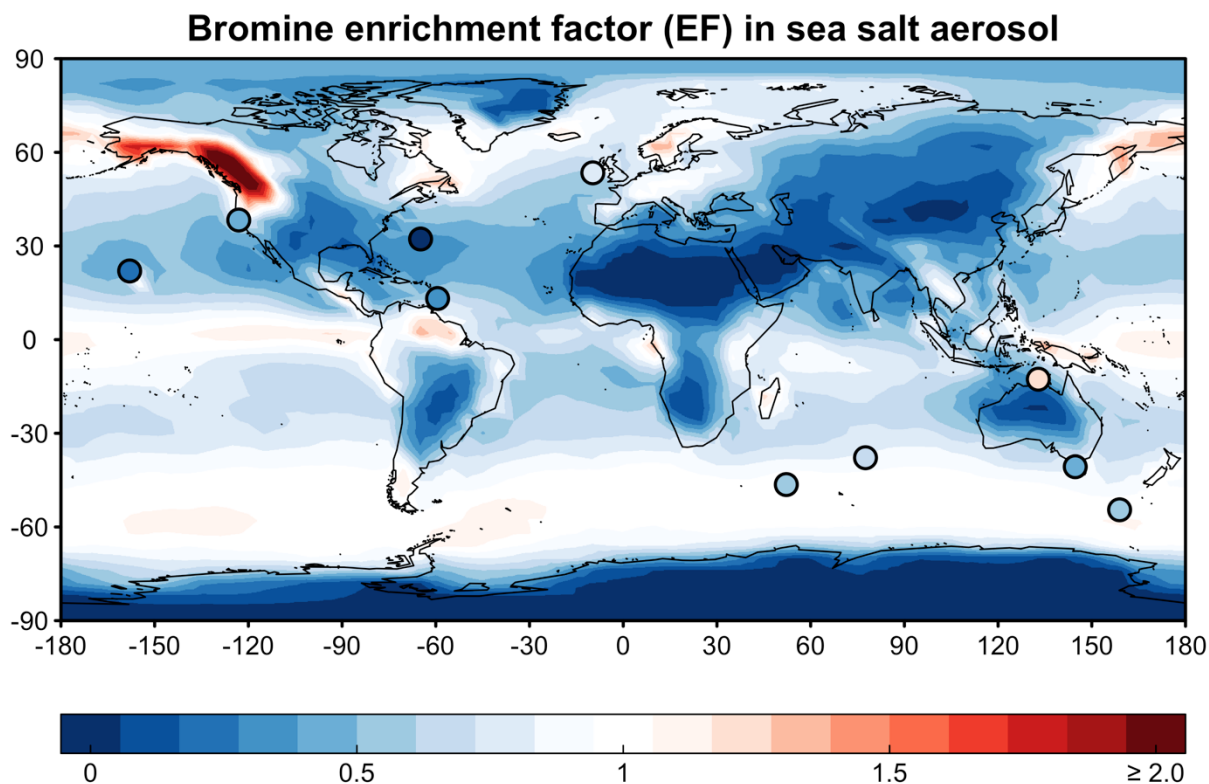
Figure 1: Annual mean bromine enrichment factor (*EF*) of sea salt aerosol in surface air simulated by GEOS-Chem. Observations at 10 sites compiled by Sander et al. (2003) and from Newberg et al. (2005) are superimposed as circles. The simulation is for 2012 and the observations are for different years. Color bar saturates at 2.0. Maximum modeled *EF* is 2.4.
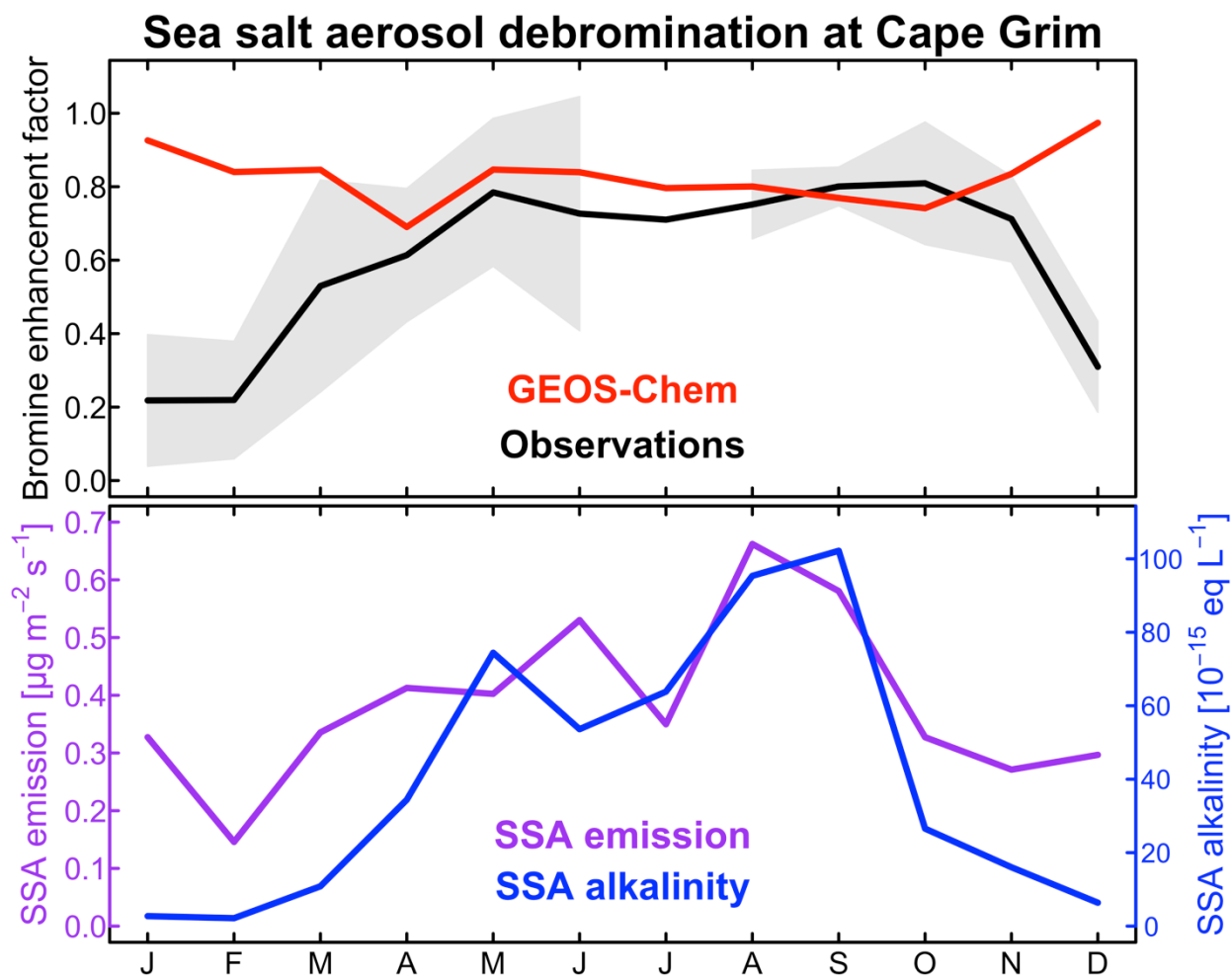
Figure 2. Seasonal variation of sea salt aerosol (SSA) debromination at Cape Grim, Tasmania (40.7°S, 144.7°E). The top panel shows the monthly bromine enrichment factors (*EFs*) of SSA in surface air. Observations from Ayers et al. (1999) and Sander et al. (2003) for 1996–1998 are compared to GEOS-Chem model values for 2012. Shading gives the interannual standard deviation in the observed monthly mean *EF* values. The bottom panel shows the GEOS-Chem monthly SSA emission flux at Cape Grim and the SSA alkalinity. The SSA emission flux is for the oceanic fraction of the Cape Grim gridsquare.
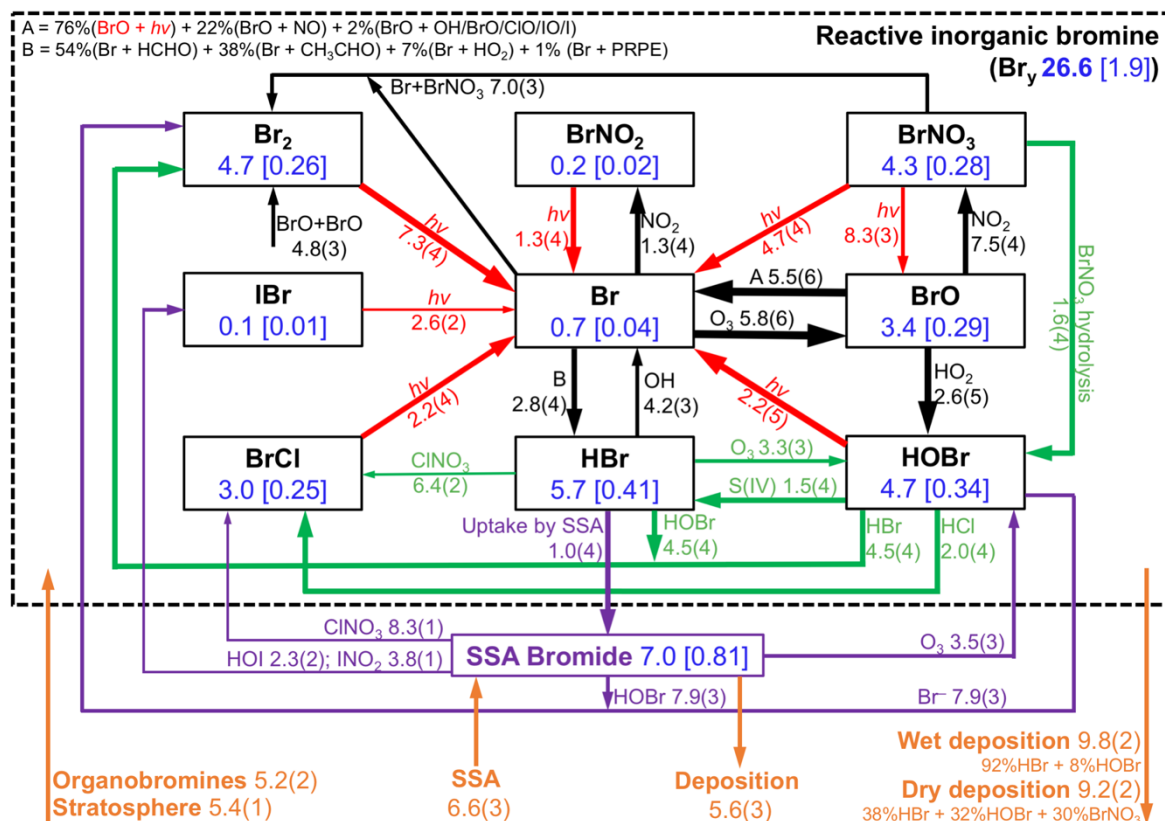
Figure 3. Global annual mean tropospheric budget and cycling of reactive inorganic bromine (Br$_y$) and sea salt aerosol (SSA) bromide. Results are from our GEOS-Chem simulation for 2012 including SSA debromination. Br$_y$ is defined as the ensemble of species inside the dashed box. Rates are in Gg Br a^{-1}, masses in the boxes are in Gg Br, and numbers in brackets are mean mixing ratios (ppt). Read 2.8(4) as 2.8×10^4 Gg Br a^{-1}. Arrows in black are for gaseous reactions, red for photolysis, purple for heterogeneous reactions in SSA, and green for other heterogeneous reactions taking place in cloud and sulfate aerosol. Sources and sinks of total inorganic bromine (Br$_y$ + SSA bromide) are in orange. Arrow thickness scales with its corresponding rate.
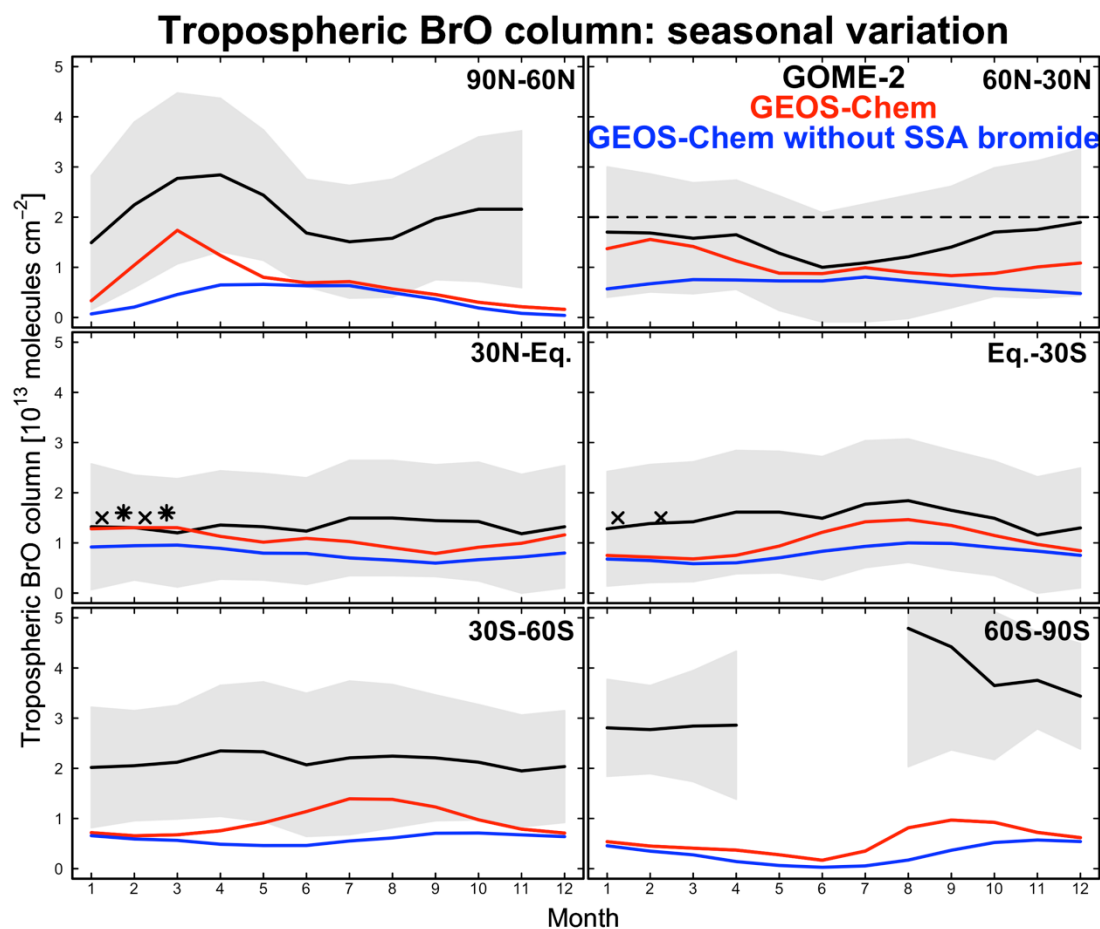
Figure 4. Seasonal variation of zonal mean tropospheric BrO columns in different latitudinal bands. Monthly GOME-2 BrO observations are for 2007 and taken from Theys et al. (2011); shading represents one standard deviation about the monthly mean GOME-2 BrO columns. GEOS-Chem BrO columns are sampled at the GOME-2 local overpass time (09:00–10:00). Red lines are from our standard simulation including sea salt aerosol (SSA) debromination, blue lines are from a sensitivity simulation without SSA debromination. The black dashed line indicates observations for 2009–2011 reported by Coburn et al. (2011) in Florida, USA without seasonality information. Black crosses and stars represent average BrO columns measured during aircraft campaigns over the eastern tropical Pacific (Volkamer et al., 2015; Wang et al., 2015; Dix et al., 2016) and western tropical Pacific (Koenig et al., 2017), respectively.
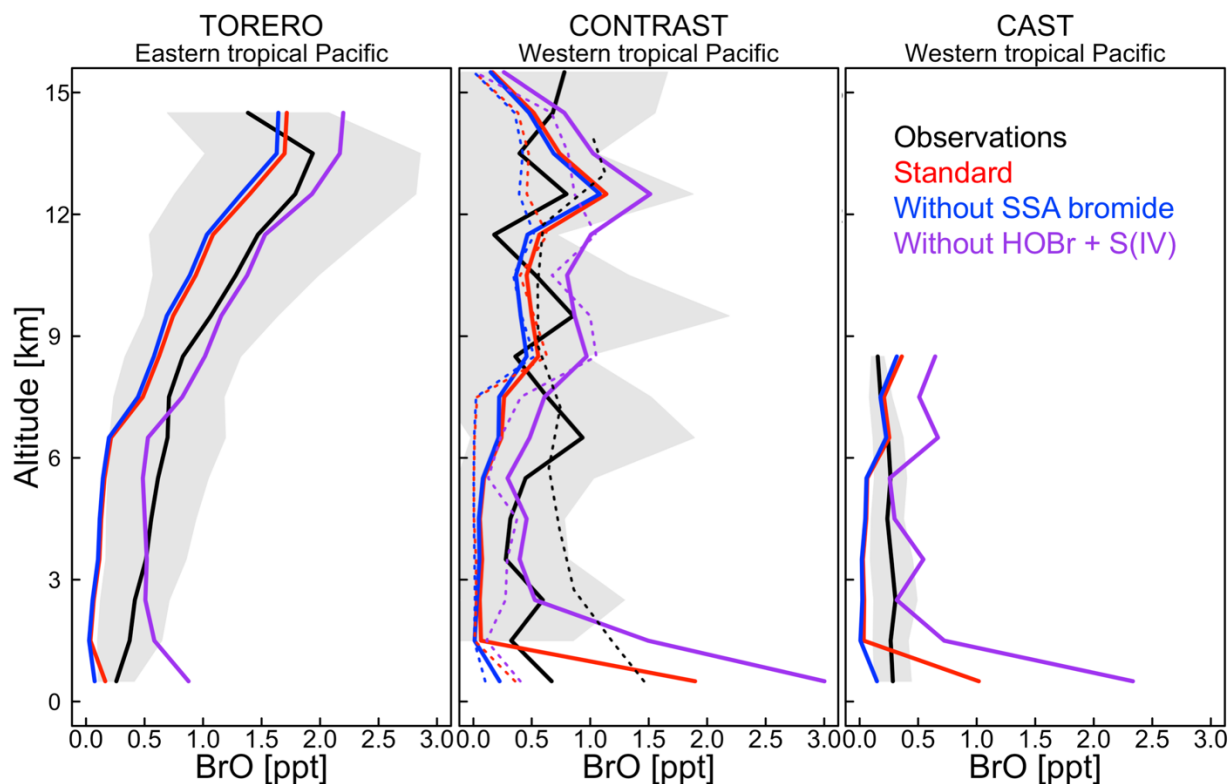
Figure 5. Vertical profiles of BrO concentrations over the tropical Pacific. Observations from the TORERO (Volkamer et al., 2015; Wang et al., 2015; Dix et al., 2016), CONTRAST (Chen et al., 2016; Koenig et al., 2017), and CAST (Le Breton et al., 2017) aircraft campaigns are compared to model values. Solid black lines indicate mean observed values in 1-km vertical bins and with standard deviations (shading). Dotted black line shows the median values as reported in Koenig et al. (2017). GEOS-Chem is sampled along the flight tracks at the time of the measurements. Model results are shown from our standard simulation including sea salt aerosol debromination (red lines), and sensitivity simulations not including SSA debromination (blue lines) and HOBr + S(IV) reactions (purple lines). Solid lines are mean values, dotted lines are median values.
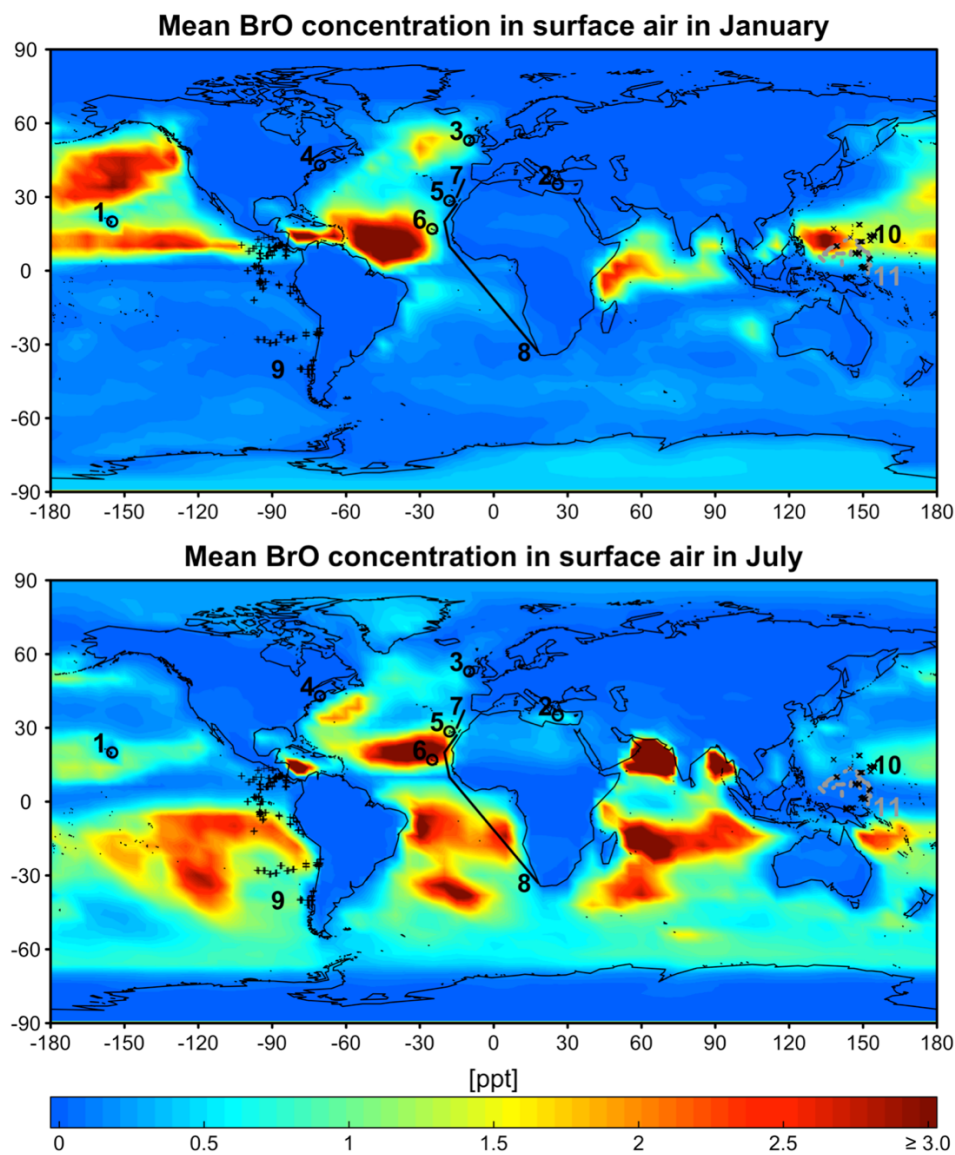
Figure 6. GEOS-Chem mean BrO concentrations in surface air in January (top) and July (bottom). Locations of BrO observations in Table 1 are shown as symbols. Open circles are ground sites and solid lines are ship tracks. Flight tracks in the marine boundary layer (< 2 km) during the TORERO (Volkamer et al., 2015; Wang et al., 2015; Dix et al., 2016), CONTRAST (Chen et al., 2016), and CAST (Le Breton et al., 2017) aircraft campaigns are shown as pluses, crosses, and dots (gray), respectively. Daytime BrO concentrations are about double the values shown here since BrO drops to near zero at night. Color bar saturates at 13.8 ppt near India.

Table 1. Daytime mixing ratios (ppt) of BrO in the marine boundary layer [a]

No.	Location	Time	Observed [b]	Simulated [c]	Reference [d]
		Ground-based measurements			
1	Hawaii (20°N 155°W)	Sep. 1999	< 2.0	0.63	1
2	Crete (35°N 26°E)	Jul.–Aug. 2000	< 0.7–1.5	0.73	1
3	Mace Head (53°N 10°W)	Apr.–Oct. [e]	< 0.3–2.5	1.3	1, 2, 3
4	Maine (43°N 71°W)	Jul.–Aug. 2004	< 2.0	0.89	4
5	Tenerife Island (29°N 17°W)	Jun.–Jul. 1997	3.0	1.9	1
6	Cape Verde (17°N 25°W)	Nov. 2006–Jun. 2007	2.5 ± 1.9	2.8	5, 6
		Ship-based measurements			
7	Atlantic Ocean (30°N–37°N)	Feb. and Oct. [f]	~ 1.0	0.91	7, 8, 9
8	Atlantic Ocean (33°S–27°N)	Oct. 2000	< 1.0–3.6	1.9	7
		Aircraft-based measurements			
9	Eastern tropical Pacific Ocean (TORERO)	Jan.–Feb. 2012	0.26 ± 0.15	0.16	10, 11, 12
10	Western tropical Pacific Ocean (CONTRAST)	Jan.–Feb. 2014	0.63 ± 0.74	1.8	13
11	Western tropical Pacific Ocean (CAST)	Jan.–Feb. 2014	0.28 ± 0.16	1.0	14

[a] Locations of measurements are shown in **Figure 6**.

[b] Values reported as ranges, means, and means ± standard deviations depending on availability. The symbol "<" indicates that
BrO is below the corresponding detection limit.

[c] Mean values for the simulated model year of 2012. The observations are for different years. Model values are sampled at the
location and time of year of the observations.

[d] 1 Sander et al. (2003), 2 Saiz-Lopez et al. (2004), 3 Saiz-Lopez et al. (2006), 4 Keene et al. (2007), 5 Read et al. (2008), 6
Mahajan et al. (2010), 7 Leser et al. (2003), 8 Martin et al. (2009), 9 Saiz-Lopez et al. (2012), 10 Volkamer et al. (2015), 11
Wang et al. (2015), 12 Dix et al., (2016); 13 Chen et al. (2016), and 14 Le Breton et al. (2017)

[e] from 1996, 1997 and 2002.

[f] from 2000 and 2007.